

Surface Modification of Gold Nanoprisms and Their Self-Assembly with Nanospheres

Dániel Zámbo, Dávid Kovács, Gergely Südi, and András Deák*

Controlled surface modification of gold particles is of central importance for the preparation of functional nano-objects, which can be used both in fundamental research and in advanced photonic or nanomedicine applications. In this study, the surface modification of gold nanoprisms using different thiols, namely cysteamine, (16-mercaptohexadecyl)trimethylammonium bromide (MTAB), and α -methoxy- ω -mercapto polyethylene glycol (mPEG-SH (5000 Da)) is investigated. The aim is to prepare binary surface-modified thiol/PEG patchy gold nanoprisms, where the tips/edges and the face regions of the particles are covered by different thiol moieties. By investigating the time evolution of the prisms' extinction spectra at different capping ligand concentration levels, the conditions to prepare such "patchy" particles are identified. While significantly faster adsorption kinetics are observed for MTAB compared to cysteamine, both molecule types can be used to prepare binary surface-modified thiol/PEG particles. Prisms modified with only MTAB or PEG and subsequently assembled with negatively charged spheres show that MTAB forms hetero-aggregates with the spheres, while PEG prevents particle attachment. For thiol (cysteamine or MTAB)/PEG binary surface-modified prisms, it is found that the efficiency of sphere attachment at the tip/side region during self-assembly is rather low, most likely due to the presence of PEG.

1. Introduction

Self-assembled nanostructures often show interesting new properties, hence controlling the arrangement of building blocks by fine-tuning their interaction at the nanoscale is of central importance.^[1] Gold nanoparticles are extensively employed for self-assembly studies, as their plasmonic properties and the assembly-related plasmon coupling enable spectroscopic investigation of the process both at the ensemble and individual particle levels.^[2,3] For wet-chemistry derived, symmetry-broken gold nanoparticles (rods, bipyramids, plates,


prisms), the shape already imposes anisotropic colloidal interaction on self-assembling systems.^[4,5] This can be effectively enhanced when nanoparticle systems are combined with polymer chemistry, allowing the preparation of colloids with structural patches.^[6–9] Such patchy particle systems are, in general, excellent model systems for studying the fundamentals of self-assembly^[10–12] and to create functional nanostructures.^[2,13,14] The inherently inhomogeneous distribution of original capping ligands (cetyltrimethylammonium bromide – CTAB or chloride – CTAC) over wet-chemistry derived gold particles' surface^[15,16] offers additional possibilities as well. Relying on this inherent inhomogeneity it has been demonstrated that partial ligand exchange on gold nanospheres, rod, or prisms can result in the formation of molecular patches, that is, region-selective surface modification of such gold particles can be achieved.^[17–19] The general idea is that when surface modifier molecules with high surface affinity are used (e.g., thiols for gold nanoparticles) at sufficiently low

concentration, more exposed surface sites (e.g., as a result of less compact coverage by the original ligands due to curvature) will be modified first.^[20] This kinetic control allows the preparation of site-selectively surface-modified particles, that in turn can enable spatial control of particle-particle interaction and hence attachments in a self-assembly process.

In this paper we investigate such a possible molecular patch formation on gold nanoprisms by employing positively charged thiols (cysteamine and MTAB) with the aim to selectively replace the original CTAC capping ligands at the high-curvature regions of the particles. We investigate how the nanoprisms' localized surface plasmon-related optical extinction spectra evolve over time upon adding the thiolated molecules to the system. The effect of both the thiol and CTAC bulk background concentration levels is investigated. The results are interpreted in terms of possible site-selective surface modification of the prism and the implication of thiol adsorption on the colloidal interactions. The findings are used to realize a two-step surface modification procedure involving the thiols and thiolated polyethylene glycol, aiming at the preparation of patchy gold nanoprisms. Finally, the surface-modified nanoprisms are self-assembled with oppositely charged spherical gold nanoparticles.

D. Zámbo, D. Kovács, G. Südi, A. Deák
Centre for Energy Research
Konkoly-Thege M. str. 29–33, Budapest 1121, Hungary
E-mail: andras.deak@ek-cer.hu

D. Kovács, G. Südi
Budapest University of Technology and Economics
Department of Physical Chemistry and Materials Science
Budafoki str. 6–8, Budapest 1117, Hungary

 The ORCID identification number(s) for the author(s) of this article can be found under <https://doi.org/10.1002/ppsc.202200197>.

DOI: 10.1002/ppsc.202200197

2. Results and Discussion

The synthesized nanoprisms have an edge length of 64 ± 5 nm, their thickness is 18.5 ± 2.5 nm (Figure 1 and Figure S1, Supporting Information). After depletion interaction assisted purification (see Experimental Section for details), the ensemble extinction spectrum has its maximum ≈ 631 nm and corresponding to the dipolar resonance of the prisms (Figure 1.c and Figure S2, Supporting Information).^[21] Spherical gold nanoparticles were prepared by the classical Turkevich method providing small nanospheres with an average diameter of 14.8 ± 1.4 nm. Surface citrate ligands were replaced by 11-mercaptoundecanoic acid (MUA) upon the addition of MUA solution and subsequent shaking at basic pH to graft the particle surfaces with permanently bound, negatively charged ligands.

2.1. Surface Modification of the Nanoprisms Using Cysteamine

The surface modification of the prisms was investigated at 100 and 10 mM CTAC background concentration levels, as it was observed earlier for gold nanorods that bulk surfactant concentration influences the ligand exchange process.^[22] Figure 2 shows the obtained results when cysteamine is applied at different concentrations in the presence of 100 mM CTAC. It is clear from the temporal evolution of the extinction spectra that the particles lose their colloidal stability, indicated by the decrease of the main peaks' extinction value and their broadening. For better visualization of the process, the time-dependent wavelength position of the dipolar resonance peak

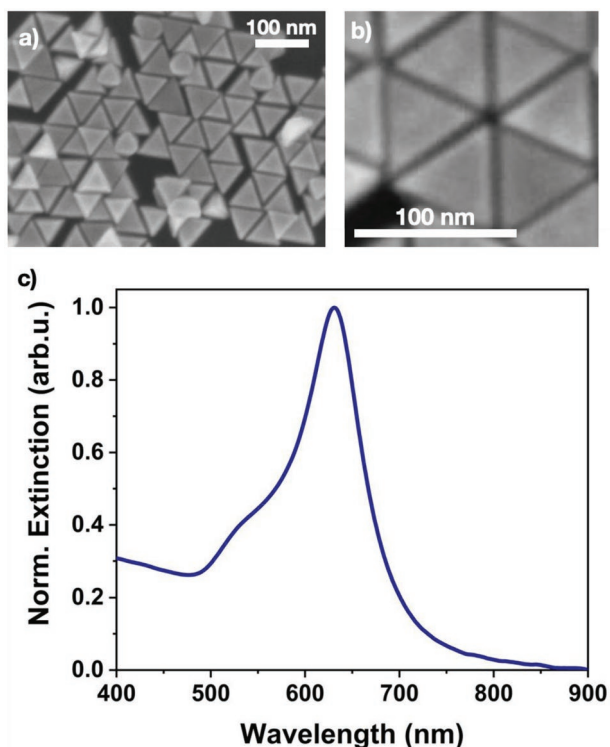


Figure 1. a,b) Scanning electron microscopy image of the nanoprism c) and their ensemble extinction spectrum after purification.

was determined as well as the extinction value at 850 nm extracted (Figure 2d–f). As a general rule, the loss of colloidal stability and the resulting particle aggregation lead to the redshift and broadening of the plasmon peak as a result of plasmon coupling.^[23,24] In spite of the obvious aggregation of the system, a clear blueshift is observed during the initial stage of the process. This blueshift is an indication of the short cysteamine molecule replacing the CTA⁺ at the particles' surface, leading to a lower effective refractive index in the optical near field and hence larger energy (shorter wavelength) plasmon resonance (Figure S2, Supporting Information).^[25] It has to be emphasized, that although thiols might etch gold nanoparticles, in the present system etching as the origin of the observed blueshift can be excluded (Figure S3, Supporting Information) even at a concentration as high as 2.5×10^{-2} M. The rate of the blueshift scales with the concentration of cysteamine, the higher its value, the faster the wavelength drop. At 10^{-3} M cysteamine concentration, the shift can only be tracked reliably in the first 8 min. The extinction intensity monitored at 850 nm shows that aggregation almost immediately takes off, but its value decreases after 15 min due to sedimentation-related removal of large aggregates from the light path (Figure 2d). At 10^{-4} M, a blueshift as large as 9 nm can be detected, whereas both the wavelength and extinction change become slower (Figure 2e). Further decreasing the cysteamine concentration to 10^{-5} M even slower kinetics is observed, the blueshift reaches only 8 nm. At the same time, however, the extent of aggregation is greatly reduced.

The loss of colloidal stability is clearly connected to the amount of cysteamine. It is well established, that gold nanoparticles prepared in the presence of CTA⁺ molecules are stabilized by repulsive electric double-layer interaction. Replacing the CTA⁺ molecules at the interface leads to a reduction of this repulsion and attractive dispersion and depletion interaction will dominate.^[26,27] As the interaction energies scale with the interacting area, if the cysteamine is assumed to evenly cover the prisms' surface the loss of stability should result in face-stacking of the plate-like particles. This is for example exploited during the depletion interaction assisted purification of the prisms,^[28] and such structures are generally observed in electron microscopy for dried-in samples.^[29] Optical calculations on dimers and larger structures indicate, that this face-stacking of the prisms might lead to some blueshift of the resonance peak as a result of developing anti-bonding modes (Figure S4, Supporting Information), but the experimentally measured spectral distortions observed in the NIR wavelength range cannot be explained in this way. The lateral (edge/tip) attachment of the prisms on the other hand (Figure S5, Supporting Information), provides a simple way to explain to observed extinction increase in the NIR wavelength range, especially as during bulk experiments a myriad of different geometrical configurations with different coupled plasmon modes might exist simultaneously. Scanning electron microscopy examples of particle aggregates also indicate a rather random aggregate morphology in contrast to the usually observed face-stacking for a native, dried-in sample (Figure S6, Supporting Information).

To reveal the effect of bulk CTAC concentration, the same cysteamine concentrations as above were used to repeat the experiments at 10 mM CTAC background concentration level.

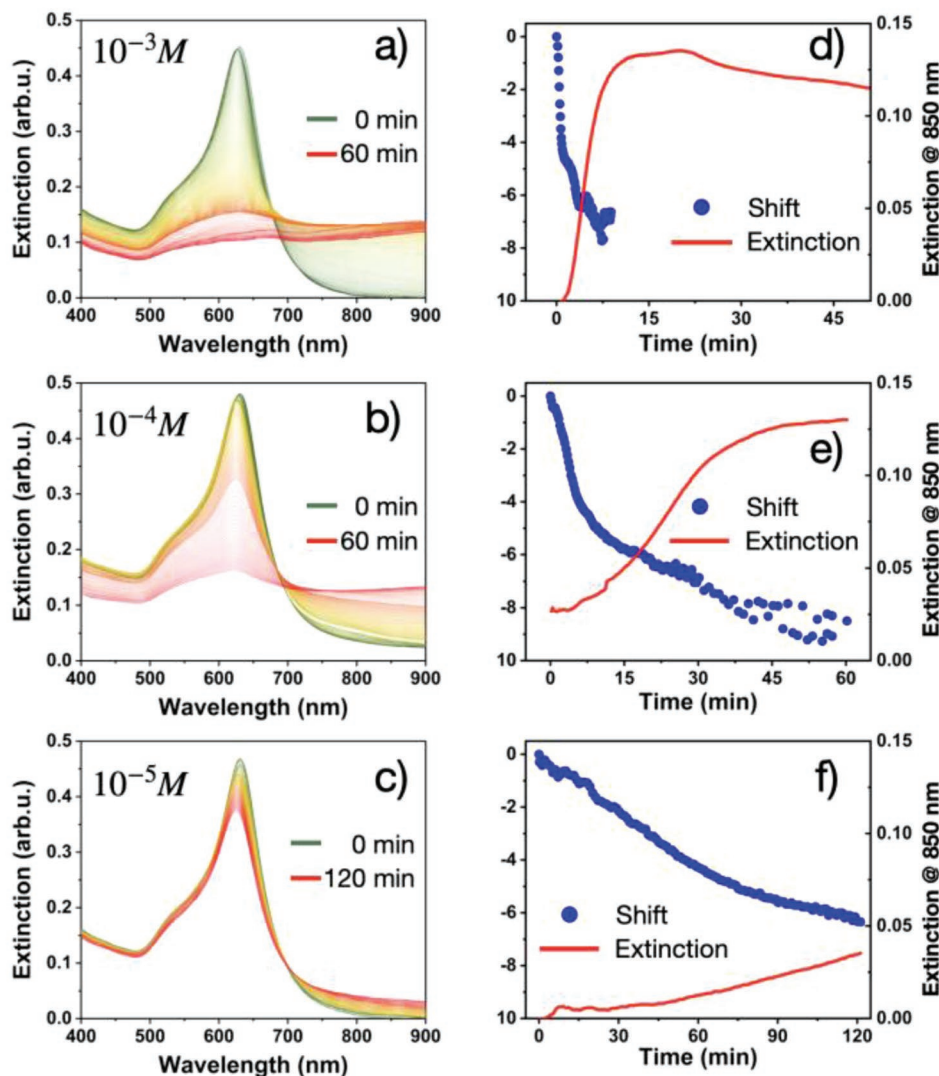


Figure 2. Temporal evolution of the nanoprisms' ensemble extinction spectrum at 100 mM CTAC bulk concentration and different cysteamine concentrations – a) 10^{-3} M, b) 10^{-4} M and c) 10^{-5} M. Figure d–f) shows the corresponding peak shifts and extinction values at 850 nm. In (d) the shift is only plotted in the first 8 min due to excessive aggregation.

As the CTAC concentration – and hence the attractive depletion interaction – is decreased, the system remains stable – neither the extinction spectra, nor the extinction measured at 850 nm indicates particle aggregation (Figure S7, Supporting Information). At the same time, however, the blueshift of the resonance peak can be still observed in all cases (Figure 3a). After 60 min, all investigated systems approach the same, ≈ 4.5 –5 nm blueshift. This can be assigned solely to replacing the CTA^+ molecules, as aggregation-related spectral changes are absent. With increasing thiol concentration, the replacement becomes faster and converges after 60 min to a similar blueshift value in each case. In the investigated cysteamine concentration range, the concentration of thiol molecules largely exceeds the nanoprism concentration (0.03 nM), and based on the total surface area of the particles estimated using the particle geometry, it would be sufficient for the full coverage of the particles' surface (Figure S8a, Supporting Information). Hence, the observed

differences in the kinetics might be attributed to the rate of adsorption being the determining step during the exchange. This is supported by the similarity of the adsorption rate constantly obtained after fitting the blueshift with a first-order kinetic curve (Figure S8b, Supporting Information). These findings indicate that there is a difference in the cysteamine coverage of the tips/edges of the prisms and face-region, which is in line with earlier findings, where site-selective surface modification of gold nanoparticles with thiolated molecules was achieved by fine-tuning the thiol concentration, as high-curvature regions of the nanoparticles are more easily accessible due to the less compact CTA^+ coating.^[19,20,30]

2.2. Surface Modification of the Nanoprisms Using MTAB

When MTAB is used for ligand replacement, two main differences are observed. In contrast to cysteamine, MTAB does

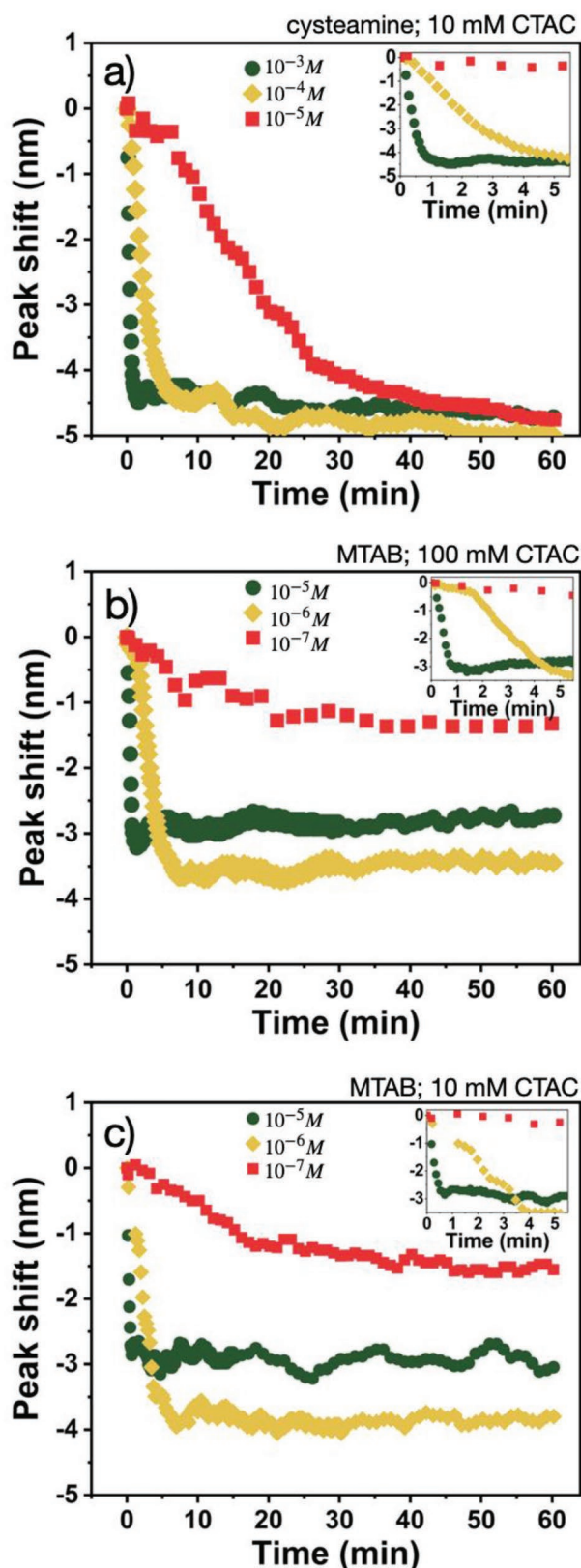


Figure 3. Time evolution of the wavelength shift using cysteamine at 10 mM CTAC (a), MTAB at 100 mM (b) and 10 mM (c) CTAC concentration. The insets show an enlarged view of the first five minutes.

allow to approach constant blueshift values (Figure 3b) without the loss of particle stability even at 100 mM CTAC background concentration (Figures S9 and S10, Supporting Information). The kinetics is, however, much faster, given that MTAB concentrations below 10^{-5} M were used. MTA⁺ is the thiolated analog CTA⁺, hence, compared to cysteamine, a rapid incorporation and exchange of MTAB in the supramolecular structures of CTA⁺ molecules in the bulk (micelles) and at the particles' surface (CTA⁺ capping layer) can be expected. This leads to a rapid blueshift in spite of the fact that MTAB concentration is 3 orders of magnitude lower, than for cysteamine. This better surface accessibility might also result in a more uniform accumulation of the thiols over the prisms' surface, as indicated by the concentration-dependent final blueshift value. It can be argued that at the highest applied concentration (10^{-5} M), a simple ligand exchange might take place. At intermediate (10^{-6} M) MTAB concentration, a slower exchange but larger blueshift is obtained, indicating that some site selectivity in the MTA⁺ accumulation at the particle surface must still apply. For the lowest investigated MTAB concentration (10^{-7} M), the blueshift reaches only ≈ 1 nm, indicating that in this case the amount of MTA⁺ molecules is simply not enough to cover the lateral regions of the particles. This is also reflected in the footprint (area/molecule) value calculated using the geometry and concentration of the nanoprisms (Figure S8a, Supporting Information), which is above that of the MTAB molecular footprint in a monolayer ($0.27 \text{ nm}^2/\text{molecule}$)^[31] at the lowest MTAB concentration. Finally, it has to be noted that in contrast to cysteamine, when MTAB is used the CTAC background level does not influence the colloidal stability of the system. This might be due to the permanent positive charge of the larger-sized MTA⁺ molecule, which seems to be sufficient to counterbalance the depletion attraction even at 100 mM CTAC concentration and hence prevent aggregation.

The particles prepared at 10 mM CTAC and intermediate thiol concentration (10^{-4} M cysteamine and 10^{-6} M MTAB) were also subjected to energy dispersive X-ray spectroscopy (EDS) measurement (Table S2, Supporting Information), which indicated that smaller amount of sulfur is present than in a fully thiolated sample, despite already these intermediate concentrations would allow for a monolayer coverage (Figure S8a, Supporting Information). As at the same time the final blueshift is obtained in these samples, the accumulation of the thiols at tips/edges should be more complete than at the prism faces.

2.3. Self-Assembly of Nanoprisms and Nanospheres

For the assembly experiments, the nanoprisms were subjected to a two-step surface modification process to amplify and solidify the eventual site-selective surface modification of the prisms by either cysteamine or MTAB. Thiolated PEG (mPEG-SH, 5000 Da) was introduced in the second step during ligand replacement at an appropriate time. mPEG-SH is a neutral polymer and is expected to attach to surface sites that are not yet occupied by smaller thiols. As the large chain length ensures significant steric repulsion that prevents nanospheres below 20 nm to assemble at larger PEGylated gold particles,^[32] this binary thiol/PEG surface grafted nanoprism

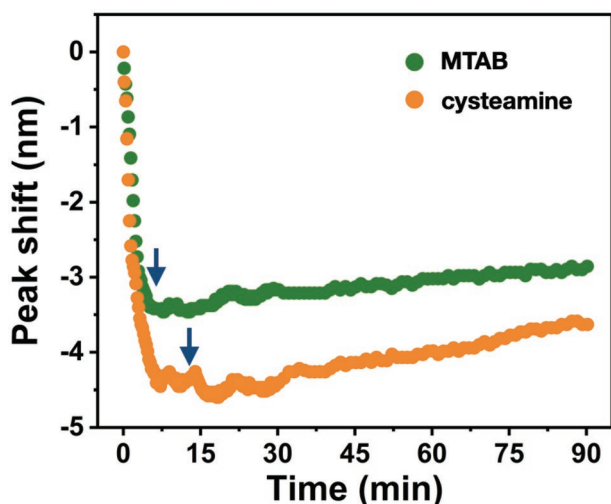


Figure 4. Peak position of the nanoprisms' extinction spectrum during the two-step surface modification using thiols and thiolated PEG (5000 Da). The arrows indicate the injection of PEG into the system (7 min for MTAB and 13.5 min for cysteamine).

can provide a platform for directed sphere/prism heteroassembly formation.

Based on the results showed earlier, the preparation of binary, thiol/PEG-coated nanoprisms was carried out at 10 mM CTAC concentration using 10^{-4} M cysteamine or 10^{-6} M MTAB and 10^{-3} M mPEG-SH, the latter being injected to the system when the blueshift reaches near its maximum value. The spectra

recorded during the two-step ligand exchange procedure are shown in **Figure 4**. In spite of the large excess of PEG present in the system, PEG is not replacing the already attached smaller thiols at the tip/edge regions. Nevertheless, its accumulation at the prisms' surface has some impact on the optical density in the prisms' dipolar mode-related near-field region, owing to the large size of the polymer molecules, resulting in a slow and moderate redshift. Based on this, the successful preparation of binary surface-modified prisms can be anticipated, where the prism edges/tips are covered by cysteamine or MTAB, and the remaining sites are occupied by PEG.

First, the self-assembly of negatively charged, MUA-coated nanospheres with fully MTAB-coated and PEGylated nanoprisms were investigated as reference samples, as for MTAB, the attractive double-layer interaction is expected to induce heteroaggregation, while for PEG, the steric repulsion of the polymer chains is expected to prevent the attachment of the spheres to the prisms. The MUA-coated nanospheres feature substantial negative electrophoretic mobility ($-2.95 \mu\text{mcm Vs}^{-1}$), while the MTAB-coated prisms show a positive value ($1.29 \mu\text{mcm Vs}^{-1}$). It has to be noted that in spite of the PEG being a neutral polymer, the PEGylated prisms have small positive mobility ($0.66 \mu\text{mcm Vs}^{-1}$), indicating the presence of residual CTA⁺ molecules, in accordance with earlier findings.^[33]

During heteroassembly, the sphere/prism ratio was set to 10. **Figure 5** shows the normalized extinction spectra recorded during the process and the SEM images of the resulting heteroaggregates. In the spectrum of the mixed system, there is also a pronounced peak ≈ 530 nm due to the presence of spherical

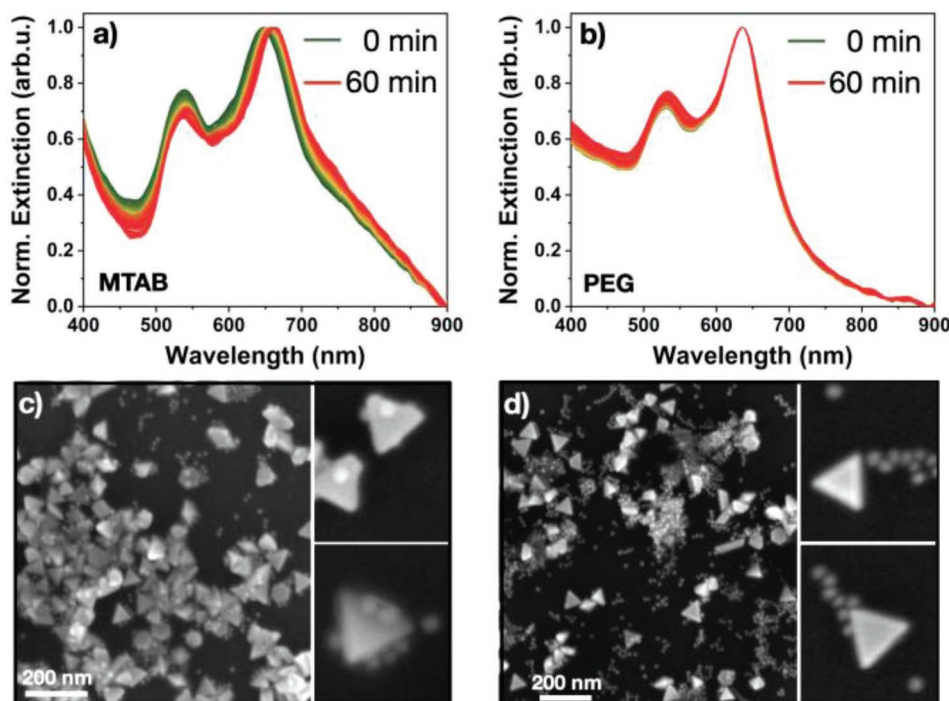


Figure 5. Normalized extinction spectra recorded during the assembly of MTAB (a) and PEG (b) coated nanoprisms with MUA-covered nanospheres; c,d) shows the corresponding SEM images of drop-casted samples together with the enlarged view of typical individual prism/sphere structures. The sphere/prism number ratio is 10/1.

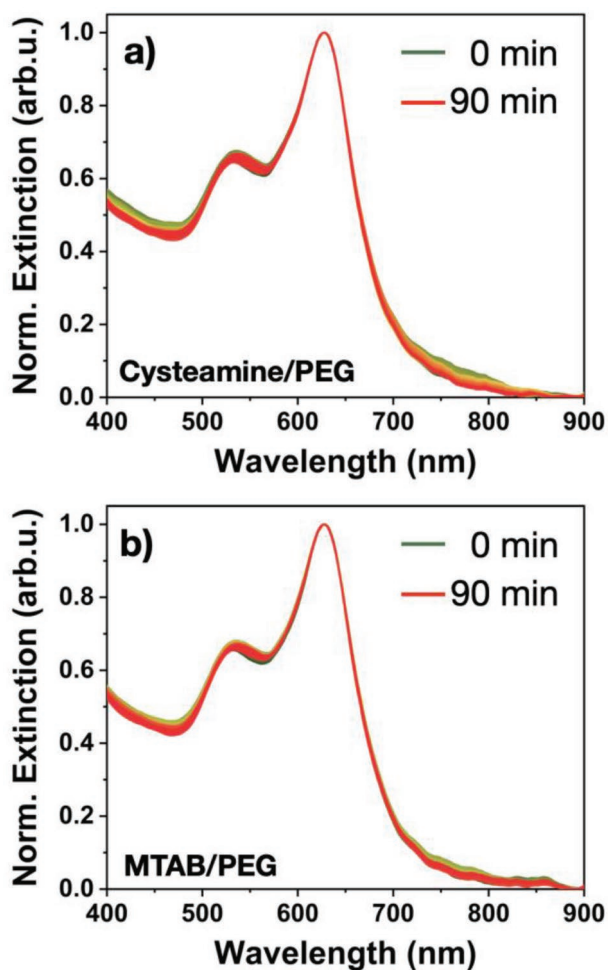


Figure 6. Normalized extinction spectra recorded during the assembly of cysteamine/PEG (a) and MTAB/PEG (b) coated nanoprisms with MUA-covered nanospheres. The sphere/prism number ratio is 10/1.

particles. For MTAB-covered particles, the dipole resonance of the prisms shows a gradual redshift with time, indicating the formation of sphere/prism heteroassemblies (Figure 5a). This is confirmed by the SEM images (Figure 5c), where the attachment of spheres to the prisms' surface is observed. In contrast to the PEGylated prisms (Figure 5b), no change in the dipole resonance is observed, only a small increase of the peak ≈ 530 nm is detected in the normalized spectra, which is a result of slow prism sedimentation, leading to an apparent increase of the sphere peak. In the corresponding SEM images (Figure 5d), the simultaneous presence of the prisms and spheres is observed without a clear tendency of the spheres attaching to the prisms. Optical simulations of sphere/prism heterodimers (Figure S11, Supporting Information) suggest that the observed redshift for MTAB might originate from spheres assembling on individual prisms, but its contribution cannot be unambiguously separated from the eventual formation of larger heteroaggregates.

Assembly has been also carried out using the hybrid, thiol/PEG-coated prisms and MUA-coated spheres (Figure 6). Both for the cysteamine/PEG and MTAB/PEG systems the results resemble the spectra obtained for the fully PEGylated system (Figure 4.b), that is, no clear spectral changes are observed, which indicates that PEG prevents excessive sphere/prism heteroaggregation in spite the presence of cysteamine or MTAB at the prism tips/edges. The attachment of spheres to the tips/edges, however, cannot be excluded a priori, given that the prism/sphere ratio is set to 1/10 and only minute changes can be expected based on calculations (Figure S11, Supporting Information).

The SEM images recorded after assembly are very similar for both the cysteamine/PEG and MTAB/PEG systems. There are some heteroassemblies found in both cases (Figure 7) with a moderate number of spheres attached to the prisms, but their occurrence is rather modest: 17% and 20% were found for the cysteamine/PEG and MTAB/PEG systems, respectively, based on checking 150 well separated individual nanoprisms. In reality, this value is most probably much lower, as most of

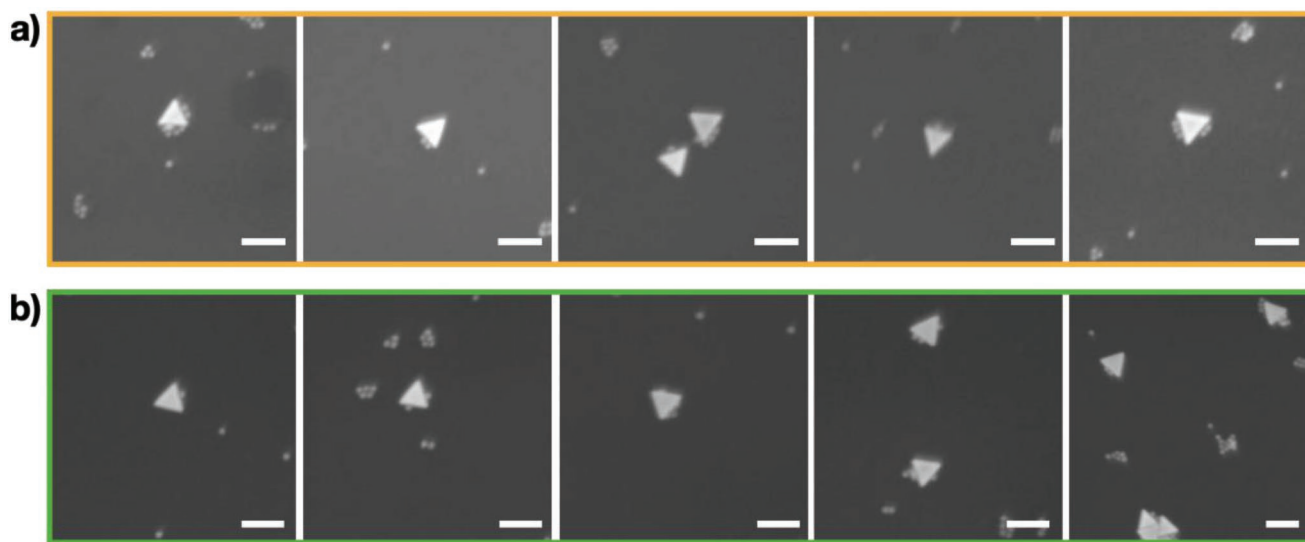


Figure 7. SEM images of individual nanoprisms featuring assembled nanospheres for the cysteamine/PEG (a) and MTAB/PEG (b) systems. The scale bar is 100 nm.

the particles can be found in the form of large dried-in agglomerates, with no clear indication of heteroaggragate formation (Figure S12, Supporting Information). This is in contrast with our earlier findings obtained on a rod/sphere system, where both bulk and interfacial assembly proved to be highly efficient and robust.^[32,34] Nevertheless the spheres are found at the tips/edges of the nanoprisms. The absence of the earlier observed prism-face bound spheres (Figure 4.c) for the MTAB/PEG system (Figure 7b) further supports that PEG effectively prevents the attachment of spheres at the prism faces.

3. Conclusion

It has been demonstrated that sequential thiol addition to gold nanoprisms can lead to the formation of binary-functionalized particles, amplifying the small difference in the original capping ligand (CTAC) distribution. The large difference in the kinetics of cysteamine and MTAB loading during ligand exchange indicates that more pronounced site-specific accumulation can be expected from molecules whose molecular structure differs significantly from that of the original capping species. During solvent-based ligand exchange reactions, in general, concentration levels are routinely varied. The presented results, however, highlight the importance of temporal control during the process as well, which can enable the preparation of nanoparticles with special surface composition. Using this approach thiol/PEG binary surface-modified prisms were prepared and could be assembled with nanospheres. While some sphere accumulation at the prisms' tip/edge region can be achieved, the efficiency of the process remains rather low, that might be improved by the use of thiolated polyions, allowing a stronger assembly driving force and fine-tuning the size of PEG at the same time.

4. Experimental Section

Nanoprism Synthesis and Surface Modification: Except for polyethylene glycol, all chemicals for the synthesis and surface modification had been purchased from Merck. The 5000 Da mPEG-SH had been obtained from Rapp Polymere GmbH. All chemicals were used as received without further purification. Ultrapure water (resistivity: 18.2 MΩcm) had been produced with Millipore EllixEssential 3 – Simplicity coupled system. All glassware had been cleaned with aqua regia, and dried in an oven after thorough rinsing with ultrapure water.

The gold nanoprisms had been prepared and purified according to already published protocols.^[28,35] The as-prepared sample contains 0.1 M CTAC, for the depletion interaction-based purification this has been increased to 0.125 M using a 25 wt.% (equals to 0.756 M) aqueous CTAC solution. The spherical nanoparticles had been synthesized according to the already published literature method.^[36] Surface modification of the spheres using mercapto-undecanoic acid (MUA) was carried out by adding 17.5 mL MUA solution (4.3 mM MUA in 0.1 M NaOH solution) to 20 mL as-synthesized sol under vigorous stirring.

Characterization Techniques: Electron microscopy was performed using a Zeiss LEO 1540 XB field-emission scanning electron microscope operated at 5 keV acceleration voltage. Samples for SEM had been prepared under ambient conditions by drop-casting and drying 1 μL solution on small silicon substrates.

A Shimadzu UV-3600i Plus spectrometer had been used for standard optical extinction spectrum measurements as well as to determine and adjust the concentration of the nanoparticles in solution to its desired value (see Supporting Information for details). For time-dependent

spectral measurements, a fiber-coupled spectrometer (stabilized tungsten halogen light source – Thorlabs SL201L, cuvette holder – Thorlabs CVH100, fiber-coupled spectrometer – Thorlabs CCS200) had been used with custom developed control software written in Labview. The plasmon peak wavelength position had been determined using OriginPro.

Optical simulation of the nanoparticles and their assemblies had been carried out in Matlab using the MNPBEM package developed by Hochenester and Trügler.^[37] The particle dimensions were used as obtained from SEM, the refractive index of the embedding medium was set to 1.3, while the dielectric function of gold was taken from Olmon et. al.^[38] Two orthogonal illumination directions with two orthogonal polarization each had been implemented and averaged.

Supporting Information

Supporting Information is available from the Wiley Online Library or from the author.

Acknowledgements

The authors thank Áron Z. Fogarasi for the assistance in the synthetic work. This work received funding from the National Research, Development and Innovation Office – NKFIH FK128327 and FK142148. Project no. TKP2021-NKTA-05 has been implemented with the support provided by the Ministry of Innovation and Technology of Hungary from the National Research, Development and Innovation Fund, financed under the TKP2021 funding scheme.

Conflict of Interest

The authors declare no conflict of interest.

Data Availability Statement

The data that support the findings of this study are available from the corresponding author upon reasonable request.

Keywords

gold nanoprisms, gold-thiol bond, optical spectroscopy, self-assembly, surface modification

Received: December 8, 2022
Published online: January 19, 2023

- [1] M. A. Boles, M. Engel, D. V. Talapin, *Chem. Rev.* **2016**, *116*, 11220.
- [2] M. Grzelczak, L. M. Liz-Marzán, *Langmuir* **2013**, *29*, 4652.
- [3] S. Pothorszky, D. Zámbo, D. Szekrényes, Z. Hajnal, A. Deák, *Nanoscale* **2017**, *9*, 10344.
- [4] G. van Anders, N. K. Ahmed, R. Smith, M. Engel, S. C. Glotzer, *ACS Nano* **2014**, *8*, 931.
- [5] D. A. Walker, E. K. Leitsch, R. J. Nap, I. Szeleifer, B. A. Grzybowski, *Nat. Nanotechnol.* **2013**, *8*, 676.
- [6] C. Hubert, C. Chomette, A. Désert, M. Sun, M. Treguer-Delapierre, S. Mornet, A. Perro, E. Duguet, S. Ravaine, *Faraday Discuss.* **2015**, *181*, 139.

- [7] R. M. Choueiri, E. Galati, H. Thérien-Aubin, A. Klinkova, E. M. Larin, A. Querejeta-Fernández, L. Han, H. L. Xin, O. Gang, E. B. Zhulina, M. Rubinstein, E. Kumacheva, *Nature* **2016**, 538, 79.
- [8] J. Kim, X. Song, A. Kim, B. Luo, J. W. Smith, Z. Ou, Z. Wu, Q. Chen, *Macromol. Rapid Commun.* **2018**, 39, 1800101.
- [9] J. Zhou, M. N. Creyer, A. Chen, W. Yim, R. P. M. Lafleur, T. He, Z. Lin, M. Xu, P. Abbasi, J. Wu, T. A. Pascal, F. Caruso, J. V. Jokerst, *J. Am. Chem. Soc.* **2021**, 143, 12138.
- [10] A. H. Gröschel, A. Walther, T. I. Löblich, F. H. Schacher, H. Schmalz, A. H. E. Müller, *Nature* **2013**, 503, 247.
- [11] A. M. Mihut, B. Stenqvist, M. Lund, P. Schurtenberger, J. J. Crassous, *Sci. Adv.* **2017**, 3, e1700321.
- [12] C. Yi, H. Liu, S. Zhang, Y. Yang, Y. Zhang, Z. Lu, E. Kumacheva, Z. Nie, *Science* **2020**, 369, 1369.
- [13] D. Rodríguez-Fernández, L. M. Liz-Marzán, *Part. Part. Syst. Charact.* **2013**, 30, 46.
- [14] C. M. Wolff, P. D. Frischmann, M. Schulze, B. J. Bohn, R. Wein, P. Livadas, M. T. Carlson, F. Jäckel, J. Feldmann, F. Würthner, J. K. Stolarczyk, *Nat. Energy* **2018**, 3, 862.
- [15] K. K. Caswell, J. N. Wilson, U. H. F. Bunz, C. J. Murphy, *J. Am. Chem. Soc.* **2003**, 125, 13914.
- [16] B. E. Janicek, J. G. Hinman, J. J. Hinman, S. hyun Bae, M. Wu, J. Turner, H.-H. Chang, E. Park, R. Lawless, K. S. Suslick, C. J. Murphy, P. Y. Huang, *Nano Lett.* **2019**, 19, 6308.
- [17] H. Duan, Q. Luo, Z. Wei, Y. Lin, J. He, *ACS Macro Lett.* **2021**, 10, 786.
- [18] Y. Yang, C. Yi, X. Duan, Q. Wu, Y. Zhang, J. Tao, W. Dong, Z. Nie, *J. Am. Chem. Soc.* **2021**, 143, 5060.
- [19] A. Kim, S. Zhou, L. Yao, S. Ni, B. Luo, C. E. Sing, Q. Chen, *J. Am. Chem. Soc.* **2019**, 141, 11796.
- [20] Z. Nie, D. Fava, E. Kumacheva, S. Zou, G. C. Walker, M. Rubinstein, *Nat. Mater.* **2007**, 6, 609.
- [21] V. Myroshnychenko, N. Nishio, F. J. García de Abajo, J. Förstner, N. Yamamoto, *ACS Nano* **2018**, 12, 8436.
- [22] D. P. Szekrényes, D. Kovács, Z. Zolnai, A. Deák, *J. Phys. Chem. C* **2020**, 124, 19736.
- [23] R. W. Taylor, R. Esteban, S. Mahajan, R. Coulston, O. A. Scherman, J. Aizpurua, J. J. Baumberg, *J. Phys. Chem. C* **2012**, 116, 25044.
- [24] G. A. Kelesidis, D. Gao, F. H. L. Starsich, S. E. Pratsinis, *Anal. Chem.* **2022**, 94, 5310.
- [25] L. Wang, M. Hasanzadeh Kafshgari, M. Meunier, *Adv. Funct. Mater.* **2020**, 30, 2005400.
- [26] J. N. Israelachvili, *Intermolecular and Surface Forces*, Academic Press, Burlington, MA **2011**.
- [27] K. Park, H. Koerner, R. A. Vaia, *Nano Lett.* **2010**, 10, 1433.
- [28] L. Scarabelli, M. Coronado-Puchau, J. J. Giner-Casares, J. Langer, L. M. Liz-Marzán, *ACS Nano* **2014**, 8, 5833.
- [29] J. Kim, X. Song, F. Ji, B. Luo, N. F. Ice, Q. Liu, Q. Zhang, Q. Chen, *Nano Lett.* **2017**, 17, 3270.
- [30] D. P. Szekrenyes, S. Pothorszky, D. Zambo, Z. Osváth, A. Deák, *J. Phys. Chem. C* **2018**, 122, 1706.
- [31] L. Vigderman, P. Manna, E. R. Zubarev, *Angew. Chem., Int. Ed.* **2012**, 51, 636.
- [32] S. Pothorszky, D. Zámbo, T. Deák, A. Deák, *Nanoscale* **2016**, 8, 3523.
- [33] A. S. D. S. Indrasekara, R. C. Wadams, L. Fabris, *Part. Part. Syst. Charact.* **2014**, 31, 819.
- [34] D. P. Szekrényes, S. Pothorszky, D. Zámbo, A. Deák, *Phys. Chem. Chem. Phys.* **2019**, 21, 10146.
- [35] L. Scarabelli, L. M. Liz-Marzán, *ACS Nano* **2021**, 15, 18600.
- [36] J. Turkevich, P. C. Stevenson, J. Hillier, *Discuss. Faraday Soc.* **1951**, 11, 55.
- [37] U. Hohenester, A. Trügler, *Comput. Phys. Commun.* **2012**, 183, 370.
- [38] S. Link, M. B. Mohamed, M. A. El-Sayed, *J. Phys. Chem. B* **1999**, 103, 3073.